JOURNAL OF MATERIALS SCIENCE 31 (1996) 2253–2264

Effects of adhesion on the effective Young's modulus in glass slide/glue laminates

Part II *Analysis*

K.-Y. LEE, E. D. CASE
Department of Materials Science and Mechanics, Michigan State University, East Lansing, MI 48824, USA

In Part I of this study we experimentally explored the effects of adhesion area, number of glue spots, and bond thickness on the effective Young's modulus in glass slide/glue composite specimens having adhesion areas ranging from 0%–100%. In this paper, the Young's modulus data are analysed further as a function of bond thickness in glass slide/glue laminates having 100% adhesion area and are compared with predictions from two existing models, a rule of mixtures model and a dynamic beam vibration model. Based on the experimental results obtained in Part I, a model has been obtained for glass slide/glue composite specimens by applying several boundary conditions. The resulting expression predicts the elastic modulus of a three-layer composite specimen bonded by an adhesive. The model developed describes well the experimental results obtained in Part I.

1. Introduction

Part I of this study [1] discussed the fabrication of the glass slide/glue composite specimens and presented empirical trends for the effects of adhesion area, bond thickness, and spatial distribution of the bond (that is, the number of glue spots). The data from Part I [1] are now analysed in terms of available models and a model is developed that is guided both by empirical results and by a consideration of physical boundary conditions on the glass slide/glue composite system.

No model is available in the literature for a laminate with a porous bond phase (corresponding to the bond phase in glass slide/glue composite specimens having adhesion areas of, say, 99% to roughly 70%) where the pores, on average, entirely penetrate the bond phase. Further, no model is available in the literature for a bond phase formed from discontinuous "islands", corresponding to the bond phase in glass slide/glue composite specimens having adhesion areas of less than about 70%. Models do exist for laminate composites having a continuous bond phase, which corresponds to a bond phase with 100% adhesion area for our glass slide/glue composite specimens. In particular, we shall use a Rule of mixtures model (ROM) and a dynamic beam vibration model to analyse the elastic modulus/bond thickness relations for those specimens having an essentially non-porous bond phase (100% adhesion area). However, neither model adequately describes the experimental modulus/bond thickness data. We then consider a model for, $E_{100}(t_R)$, the dependence of Young's modulus, E, on the relative glue bond thickness, t_R, still for the special case of 100% adhesion area. By considering various physical boundary conditions, the expression for $E_{100}(t_R)$ is subsequently extended to a semiempirical model for $E(X, t_R)$, which also describes specimens having adhesion areas less than 100 percent.

In the next two sections of this paper, we briefly review the assumptions and results for the Rule of Mixtures model and Dynamic Modulus Model. The glass slide/glue composite specimens used in the experimental study in Part I [1] can be considered as a three-layer composite composed of two slide glasses and adhesive.

1.1. Rule of mixtures (ROM) model

Assuming (1) perfect interfacial bonding between layers, and (2) linear elastic behaviour of each layer under a unidirectional load, we can express the effective elastic modulus of the three-layer composite, $\bar{E}_{3ROM}$, in terms of the elastic moduli, E, and volume fractions, V, of each layer such that (Fig. 1) [2]

$$\bar{E}_{3ROM} = E_{L1}V_{L1} + E_{L2}V_{L2} + E_bV_b \quad (1)$$

where subscripts L1 , L2 and b refer to layers 1, 2 and bond layer, respectively. The ROM model for the effective modulus is quite simple and thus can be thought of as essentially a "zeroth order" model for the laminate composites. Thus we shall use the ROM model as one point of comparison with the data. In addition to the ROM model, we shall compare our

0022–2461

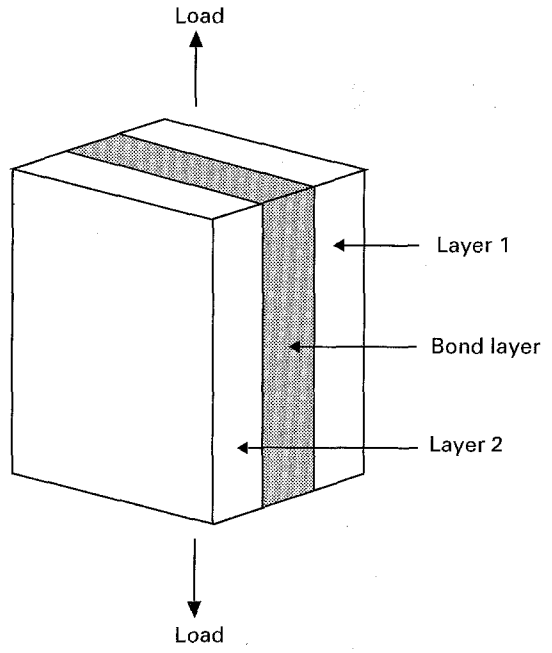

Figure 1 The three-layer composite specimen for the rule of mixtures model [2], where uniaxial tension is assumed. For this study, layers 1 and 2 were glass microscope slides.

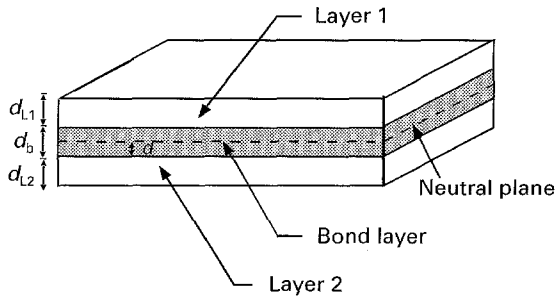

Figure 2 The three-layer composite specimen for the dynamic beam vibration model [2], where the specimen is driven at flexural resonance to determine the elastic modulus. As in Fig. 1, layers 1 and 2 were glass microscope slides for this study.

experimental data with a dynamic modulus model based on the Euler beam-bending equation.

1.2. Dynamic beam vibration model

Free, undamped vibrations of a monolithic bar can be approximated by the Bernoulli–Euler beam equation [3,4]. Applying the Bernoulli–Euler equation to a three-layer composite in which a bond layer is sandwiched between layers 1 and 2 (Fig. 2) and assuming perfect interfacial bonding between layers 1 or 2 and the bond layer, the effective elastic modulus, $\bar{E}_{3DYN}$, of a three-layer composite is given by [2–6]

$$\bar{E}_{3DYN} = \frac{(E_{L1} I_{L1} + E_{L2} I_{L2} + E_b I_b)}{(I_{L1} + I_{L2} + I_b)} \quad (2)$$

where E and I are the Young's moduli and the second moments of inertia of the cross-section of the bar with respect to the neutral axis. Subscripts L1 , L2 and b denote layer 1, layer 2, and the bond layer, respectively.

2. Analysis of glass slide/glue composite data

2.1. Comparison of observed bond thickness effects with rule of mixtures and dynamic beam vibration models

The rule of mixtures and the dynamic beam vibration models were compared to experimentally determined modulus data for 13 glass slide/epoxy resin composite specimens having a 100% adhesion area. A bond layer composition of 50% resin and 50% hardener was used for each of the 13 specimens to be consistent with the bond layer composition for the epoxy resin adhered specimens included in this study which have adhesion areas less than 100%.

The elastic moduli of the glass slide/epoxy resin composite specimens were calculated using the measured elastic moduli of the glass slides, the measured glue bond modulus, and the measured dimensions of the 13 actual specimens using Equation 1 for the ROM model and using Equation 2 for the dynamic beam vibration model. The fundamental dependence on the relative bond thickness for the moduli calculated from Equations 1, 2 and the measured Young's moduli (Fig. 3) was explored via a least-squares fit to

$$E_{100}(t_R) = A_1 + A_2 t_R \quad (3)$$

where E_{100} is the elastic modulus (GPa) for composite specimens having 100% adhesion area, A_1 and A_2 are constants (Table I). The relative thickness of the glue bond, t_R, is defined as a ratio of glue bond thickness to total thickness of glass slide/glue composite specimen. Thus over the experimental range of t_R, the ROM model, the dynamic modulus model, and the experimental data can each be described by a linear function in t_R (Fig. 3).

The measured Young's modulus decreased linearly from approximately 70.5 GPa at a relative bond thickness near 0 to a modulus of about 66.5 GPa at a relative bond thickness of 0.12 (Fig. 3). The linear decrease predicted by the ROM model was more rapid than that observed experimentally, with a ROM-predicted value of about 62.5 GPa at $t_R = 0.12$. The modulus predicted from the dynamic modulus model is relatively insensitive to the relative glue bond thickness (Fig. 3).

The relative differences, δ_R, between the experimentally determined Young's modulus, E_{exp}, and the predicted Young's modulus, E, for both the ROM (Equation 1) and the dynamic beam vibration (Equation 2) models were calculated as

$$\delta_R = \frac{(E - E_{exp})}{E_{exp}} \quad (4)$$

The δ_R versus t_R relations (which show opposite slopes for the ROM and dynamic beam vibration models) were fit to the relationship

$$\delta_R = B_1 + B_2 t_R \quad (5)$$

where B_1 and B_2 are fitting constants (Table I) (Fig. 4).

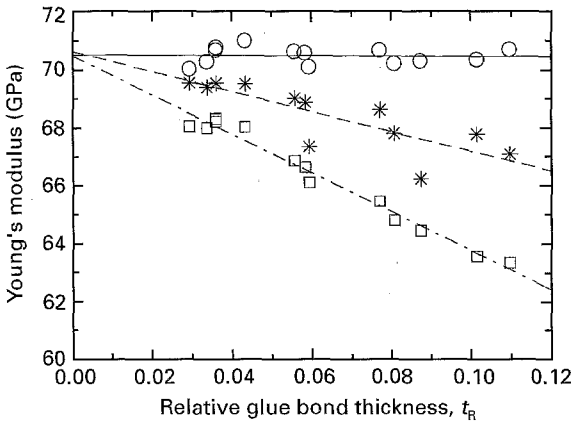

Figure 3 Comparison of (*) experimentally determined moduli with the moduli predicted from the (□) rule of mixtures and (○) dynamic beam vibration models. The comparison is made as a function of relative glue bond thickness for an epoxy resin bond composition of 50% resin and 50% hardener. The curves represent a least-squares best-fit to Equation 3.

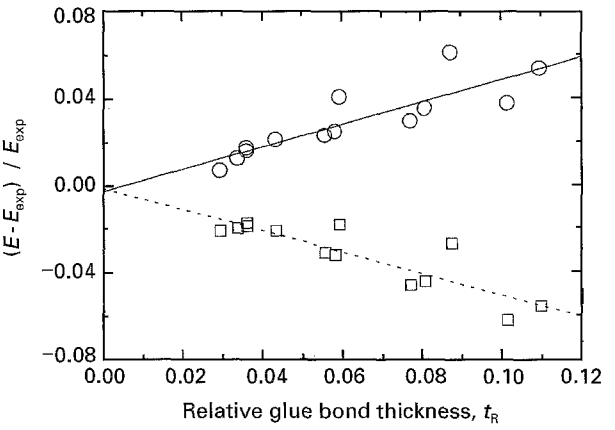

Figure 4 Comparison of the (□) ROM and (○) dynamic modulus models for epoxy bonds made from an initial composition of 50% resin and 50% hardener. The curves represent a least-squares best-fit to Equation 5.

As the relative glue bond thickness increases from 0 to about 0.12, $|\delta_R|$ for both the dynamic modulus model and the ROM model increases from 0% to about 6% (Fig. 4). Thus it is only in the limit that the relative glue bond thickness approaches zero that both models describe the Young's modulus of the three-layer composite. The best fit curves for the deviation, δ_R, have similar slopes for the two models but the opposite algebraic signs. Thus, we began our analysis by comparing data for our glass slide/glue composite specimens with calculations based on the ROM and dynamic modulus relations. We found that neither the ROM model nor the dynamic modulus model describes the modulus/glue bond thickness data for the glass slide/glue composite specimens having an adhesion area of 100%.

2.2. Development of model for glass slide/glue composite specimens

As shown in Part I [1] (Equation 2), a least-squares best-fit of the effective modulus data for the glass slide/glue composite specimens to the equation

$$E(X,t_R) = E_{100}(t_R)(1 - C_1 X^{C_2}) \quad (6)$$

yielded correlation coefficients for the various data sets that ranged from 0.97–0.99 (Table V, Part I [1]). As in Part I [1], $E(X,t_R)$ is the effective elastic modulus as a function of X (where $X = 1 - A$, and A is the fractional adhesion area), and t_R is the ratio of glue bond thickness to total composite specimen thickness. C_1 and C_2 are least-squares fitting constants, and $E_{100}(t_R)$ is the value of the effective Young's modulus of the composites for an adhesion area of 100%.

In Part I [1], $\langle E_{100}(t_R)\rangle$ was estimated directly from the measured elastic modulus data, that is, $\langle E_{100}(t_R)\rangle$ was the average of the elastic modulus data for specimens having adhesion area greater than 90% (Table IV, Part I [1]). However, the effective elastic modulus for a composite specimen having 100% adhesion area can be described as a linear function of the relative bond thickness ranging from 0 to 0.12 by Equation 3 (Section 2.1)

$$E_{100}(t_R) = A_1 + A_2 t_R \quad (3)$$

While Equation 3 does fit the experimental data over the observed relative bond thickness range ($0 < t_R < 0.12$), it is not consistent with the physical boundary conditions, for example, in the limit of $t_R = 1$ (i.e. bond layer only) while the ROM and dynamic modulus models are consistent with the physical boundary conditions (Fig. 5a). Assuming perfect bonding between the bond layer and glass slides, as the relative bond thickness goes to zero (i.e. no glue between two glass slides), the elastic modulus for a composite specimen having 100% adhesion area, E_{100}, should equal the elastic modulus for a glass slide, E_g, that is,

$$E_{100}(t_R \to 0) = A_1 = E_g \quad (7)$$

On the other hand, as the relative bond thickness, t_R, approaches unity (i.e. bond layer only), E_{100} should equal the elastic modulus for the bond layer itself, E_b,

TABLE I Fitting constants, A_1, A_2 (Equation 3), B_1, and B_2 (Equation 4), and correlation coefficients for the ROM model, experimental data, and dynamic modulus model

	A_1 (GPa)	A_2 (GPa)	Correlation coefficient	B_1	B_2	Correlation coefficient
Rule of mixtures model	70.5	−67.0	0.99	−0.0012	−0.496	0.87
Experimental data	70.6	−34.2	0.83	–	–	–
Dynamic modulus model	70.5	−0.433	0.04	−0.0025	0.511	0.86

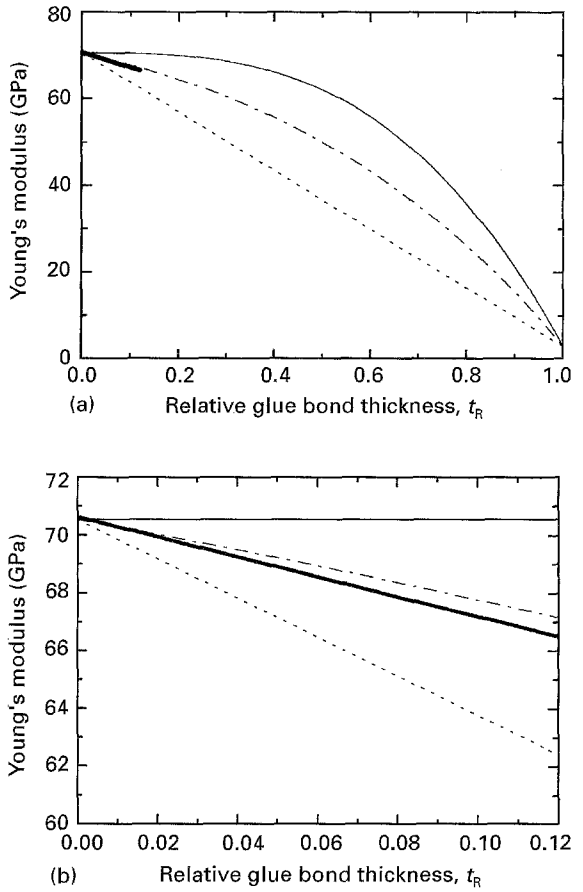

Figure 5(a) Comparison of the (– – –) ROM and (——) dynamic modulus models for the entire range of relative bond thickness. (▬) Least-squares best-fit to the experimental data shown in Fig. 3. (- — -). The Young's modulus calculated from Equation 11. (b) Detail of (a) within the range of relative bond thickness from 0–0.12 which was measured for the epoxy resin adhered composite specimens having 100% adhesion area. (▬) A least-squares best-fit of the data to Equation 3.

that is,

$$E_{100}(t_R \rightarrow 1) = E_g + A_2 = E_b \quad (8)$$

Thus

$$A_2 = E_b - E_g \quad (9)$$

Therefore, the elastic modulus for a composite specimen having 100% adhesion area can be expressed as

$$E_{100}(t_R) = E_g + (E_b - E_g)t_R \quad (10)$$

This equation is equivalent to the rule of mixtures model (Equation 1) if we assume $E_{L1} = E_{L2} = E_g$.

The elastic moduli measured for relative bond thicknesses from 0–0.12 fall between the predicted moduli from the rule of mixtures and the dynamic modulus models (Fig. 3). A number of possible physical mechanisms might explain the differences between the ROM model, the dynamic modulus model and the measured moduli (Appendix 1). However, empirically, if we multiply the second term of Equation 10 by $\exp(t_R)$, the resulting relation fits the $E(t_R)$ data relatively well. The 1/exp(1) factor is included to satisfy the boundary conditions for $t_R \rightarrow 1$

$$E_{100}(t_R) = E_g + (E_b - E_g)t_R \frac{\exp(t_R)}{\exp(1)} \quad (11)$$

In Equation 11, E_g was set equal to 70.53 GPa, the average elastic modulus measured for individual glass slides, and E_b was set equal to 3.0 GPa, the measured elastic modulus for an epoxy resin (Table II, Part I [1]). If we designate the E_{100} value calculated from Equation 11 as E_{100}(cal) and the mean of the measured E_{100} data as $\langle E_{100}(\text{exp})\rangle$, then E_{100}(cal) and $\langle E_{100}(\text{exp})\rangle$ agree to within ±1%, except for the thickest of the epoxy resin specimens, where the difference is about 1.5% (Table II).

For laminate composites with 100% adhesion area, a comparison of the effective moduli calculated by the (i) ROM model, (ii) dynamic modulus model, and (iii) Equation 11, shows that the ROM model (dotted curves in Fig. 5a and b) underestimates the measured effective modulus, the dynamic modulus model (solid curves in Fig. 5a and b) overestimates the modulus, while Equation 11 (dot-dash curve in Fig. 5a and b) agrees relatively well with the measured elastic modulus as a function of the relative bond thickness, t_R. Furthermore, for the entire physically meaningful range of t_R, that is, $0 \leq t_R \leq 1$, the modulus calculated via Equation 11 is bracketed in a symmetrical manner by the dynamic modulus estimate and the ROM estimate. For both the ROM and dynamic modulus calculations, a total specimen thickness of 2.5 mm was assumed, which was in fact typical thickness for glass slide/epoxy resin composite specimens employed in

TABLE II Comparison of E_{100}(cal) calculated from Equation 11 and experimentally determined E_{100}(exp) for each set of data. E_{100}(cal) values are calculated using the average values of relative bond thickness, t_R, for each data set specified

Adhesive type	Number of glue spots per specimen	E_{100}(cal) (GPa)	$\langle E_{100}(\text{exp})\rangle$ (GPa)	$[E_{100}(\text{cal}) - \langle E_{100}(\text{exp})\rangle]/\langle E_{100}(\text{exp})\rangle$
Super glue	1	70.35	69.99	0.51%
	2	70.35	69.99	0.51%
	3	70.38	69.99	0.56%
	5	70.38	69.99	0.56%
Epoxy cement	1	69.55	70.07	−0.74%
	3	69.92	70.07	−0.21%
Epoxy resin	3[a]	68.92	68.49	0.63%
	3 (R1[b])	70.00	69.54	0.66%
	3 (R2[b])	69.06	68.42	0.94%
	3 (R3[b])	68.05	67.03	1.52%

[a] Entire epoxy resin adhered composite specimens with bond thicknesses ranging from 0.036–0.370 mm.
[b] Ranges of bond thickness: R1, 0.025–0.075 mm; R2, 0.125–0.175 mm; R3, 0.225–0.275 mm.

this study. The specimen thickness is used in the numerical computation of volume fractions in Equation 1 (ROM model) and the second moments of inertia in Equation 2 (dynamic modulus model).

Equation 11 still satisfies the boundary conditions (Equations 7 and 8) for the two limits of the relative bond thickness ($t_R = 0$ and $t_R = 1$). Substituting Equation 11 into the empirical equation for the adhesion effect on effective elastic modulus (Equation 6), we obtain

$$E(X, t_R) = \left[E_g + (E_b - E_g)\, t_R \frac{\exp(t_R)}{\exp(1)}\right](1 - C_1 X^{C_2}) \tag{12}$$

As an additional boundary condition, if the fractional unadhered area, X, goes to 1 and t_R goes to 0 simultaneously (i.e. no glue bond layer between the two glass slide layers), then the effective elastic modulus, E, should approach the elastic modulus for a pair of glass slides having no glue bond (i.e. 0% adhesion area), E_0, such that

$$E(X \to 1, t_R \to 0) = E_g(1 - C_1) = E_0 \tag{13}$$

Thus

$$C_1 = 1 - \frac{E_0}{E_g} \tag{14}$$

and therefore, Equation 12 becomes

$$E(X, t_R) = \left[E_g + (E_b - E_g)\, t_R \frac{\exp(t_R)}{\exp(1)}\right] \times \left[1 - \left(1 - \frac{E_0}{E_g}\right) X^{C_2}\right] \tag{15}$$

Thus Equation 15 is consistent with the described boundary conditions (Equations 7, 8 and 13).

For the unadhered pairs of glass slides, E_{un}, the measured modulus is 20.04 ± 1.62 GPa (Part I, Section 3.1 [1]), which probably reflects, at least in part, frictional interaction between the glass slides. As the frictional forces between glass slides increase, the effective bond strength between the two unadhered slides should increase. Such frictional interactions no doubt depend on the detailed nature of the glass surfaces themselves and the loads applied to the specimen while performing the modulus measurements. However, the relative importance (if any) of frictional contributions to the value of E_{un} has not been demonstrated experimentally and is a topic for future study.

E_{un}, the elastic modulus for the unadhered glass slides should provide an experimental estimate for E_0, the effective modulus in the limit that the bond thickness and adhesion area approach zero simultaneously (Equation 13). Using the low adhesion area fraction data (adhesion areas less than 15%, as shown in Fig. 6a for the specimens adhered by a single glue spot) one can estimate E_0 by extrapolating the experimental modulus data to zero adhesion area. The E_0 obtained by this extrapolation ranges from about

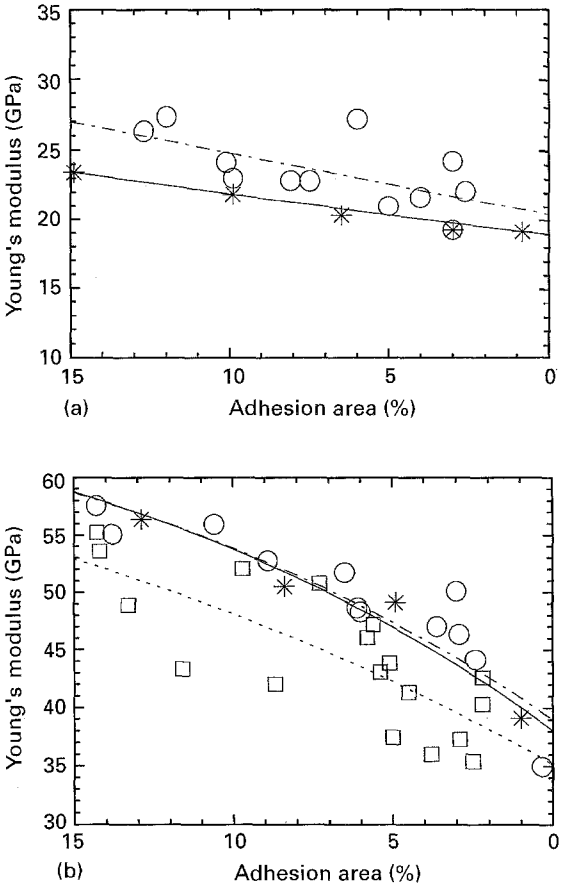

Figure 6(a) Estimation of E_0 for (○) super glue and (*) epoxy cement for one glue spot adhered composite specimens. (b) Estimation of E_0 for (○) super glue, (*) epoxy cement and (□) epoxy resin three glue spot adhered composite specimens. Each curve represents a least-squares fit to the empirical power-law expression (Equation 2) in Part I [1].

19.0–20.5 GPa, which agrees well with the measured E_{un} value of 20.04 ± 1.62 GPa. In contrast to the measured E_{un} values and E_0 values determined by extrapolating the single glue spot data, extrapolations of the multiple glue spot data for low adhesion area fractions (Fig. 6b) gives E_0 values that range from about 35.0–40.0 GPa. The physical mechanisms that give rise to the difference between the E_0 values estimated for the multiple and single glue spot data are not known, although Appendix 2 suggests possible mechanisms that might lead to the observed differences in E_0.

2.3. Selection of power-law exponent and E_0 values for the modulus model

It was our goal to obtain an expression for $E(X, t_R)$ that involved a single integer numerical value for the exponent C_2. Given the power-law equation embodied by Equation 15, it was not possible to find a single integer value for exponent C_2 to describe adequately all the data. However, an exponent of $C_2 = 5$ fit all of the multiple glue spot data well and an exponent of $C_2 = 2$ was adequate for the data from specimens adhered by a single glue spot. We believe that the differing C_2 values are due to different physical mechanisms dominating in one glue-spot or

TABLE III Summary of statistical tests of agreement between the data and Equation 15

Number of glue spots	Super glue				Epoxy cement		Epoxy resin			
	1	2	3	5	1	3	3	3 (R1[a])	3 (R2[a])	3 (R3[a])
$\varkappa^2$	12.774	0.389	2.552	0.114	5.636	0.518	9.066	0.665	0.811	0.983
Average residual (%)	7.7	1.4	2.4	0.9	11.0	2.5	3.8	2.3	2.8	3.8
Maximum residual (%)	24.1	3.9	18.6	2.5	26.4	5.7	13.0	4.6	7.6	6.6
Minimum residual (%)	0.002	0.1	0.05	0.1	0.4	0.04	0.04	0.04	0.07	0.8
Number of data	36	21	32	13	11	10	70	15	12	10
Number of residual > 5%	20	0	3	0	7	1	25	0	2	3
Number of residual > 10%	14	0	2	0	5	0	4	0	0	0
Number of sign runs	6	7	9	4	2	5	22	6	3	2

[a] Ranges of bond thickness: R1, 0.025–0.075 mm; R2, 0.125–0.175 mm; R3, 0.225–0.275 mm.

multiple glue-spot adhered composite specimens (see Appendix 2).

The optimum C_2 value was determined by calculating the value of $\varkappa^2$

$$\varkappa^2 = \sum_{i=1}^{k} \frac{(O - e)^2}{e} \tag{16}$$

where O and e denote an observed value and the corresponding expected value, k is the number of data items in each data set, and $\varkappa^2$ measures the overall goodness of fit between the data and a given model. The optimum exponent C_2 was assumed to be the C_2 value that gave the minimum $\varkappa^2$ value. $\varkappa^2$ values, the magnitude of the residuals (the difference between experimental and predicted values) as well as the number of sign runs* were calculated for C_2 values of 2, 3, 4, 5, and 6 and from this analysis we determined that $C_2 = 2$ was the optimum coefficient for the one glue spot data and $C_2 = 5$ was the optimum coefficient for the multiple glue spot data (Table III). For each set of composite specimens a value for E_0 was calculated from the measured data. For the super glue and epoxy cement single glue spot data, E_0 values were calculated from Equation 15 using $E_g = 70.53$ GPa, $E_b = 2.98$ GPa (Section 2.2) and the measured t_R and X values for each specimen (recall that $X = 1 - A$, and A is the adhesion area fraction). The E_0 value listed in Table IV corresponds to the calculated E_0 value that gives the minimum $\varkappa^2$ value. This procedure was repeated for multiple glue spot data, using Equation 15 (Table IV).

In Equation 15, the elastic modulus for a single glass slide, E_g, is 70.53 GPa which was measured in this study (Part I, Section 3.1 [1]). The value for the elastic modulus of bond layer, E_b, was measured for the epoxy resin, which was 2.98 GPa (Part I, Section 3.1, [1]). E_b for the super glue and the epoxy cement was not measured in this study and the detailed chemical compositions of the super glue and epoxy cement were unknown. Although several references [7–11] give the shear strength, tensile strength, and peel strength of specific adherends bonded by specific adhesives, very little mechanical information is given about adhesives themselves. From elastic modulus values known for several adhesive types (Table V) the elastic modulus values of the super glue and the epoxy cement probably is not greater than 10 GPa. An E_b of 10 GPa (rather than the assumed E_b value of 2.98 GPa) does not make a significant difference in the effective Young's modulus calculated by Equation 15 within the observed range of bond thickness for any of the "candidate" values of C_2 (namely 2–6) considered in this study. For example, for the values of E_g and E_0

TABLE IV E_0 and average t_R values for each set of composite specimens

Adhesive type	Number of glue spots per specimen	Number of specimens	Average t_R	E_0 (GPa)
Super glue	1	36	0.007	15.2
	2	21	0.007	44.3
	3	32	0.006	41.0
	5	13	0.006	46.7
Epoxy cement	1	11	0.038	13.2
	3	10	0.024	39.6
Epoxy resin	3	70	0.061	34.0
	3 (R1[a])	15	0.021	38.8
	3 (R2[a])	12	0.056	32.6
	3 (R3[a])	10	0.091	27.4

[a] Ranges of bond thickness: R1, 0.025–0.075 mm; R2, 0.125–0.175 mm; R3, 0.225–0.275 mm

*The number of sign runs equals the number of times the algebraic sign of the residuals changes for a given data set. Thus, the number of sign runs gives, for example, the number of times the data switch from "above" the predicted line to "below" the predicted line.

TABLE V Reference values for elastic moduli of various adhesives

Adhesive type	Measurement temperature (°C)	Elastic modulus (GPa)	Reference
Acrylo-nitrile rubber + phenolic resin	− 20	2.544	[10]
	82	0.268	
	150	0.222	
Polyurethane + hardener	− 40	0.177	[10]
	20	0.095	
	120	0.026	
Phenolic-polyvinyl formal	–	3.300	[10]
Vinyl-phenolic	–	2.241	[11]
Nylon-epoxy	–	1.241	
Epoxy-phenolic	–	2.724	
Epoxy-paste	–	3.503	
Cured epoxy resins	–	2.7–4.1	[12]
Epoxy resins	–	3.0–6.0	[13]

assumed for a glass slide/super glue composite specimen adhered by three glue spots, and t_R and X values of 0.006 and 0.8, respectively (Table IV), changing E_b from 2.98–10 GPa changes the resulting value of $E(X, t_R)$ by about 0.03%.

To illustrate the fit of Equation 15 to the data, we could plot a three-dimensional plot with axes E, X, and t_R. While we present two such plots in Section 2.4, it is difficult to obtain a detailed understanding of the differences between the data and the model equations from a three dimensional plot. Therefore, in Figs 7 and 8 we plot E_{cal}, the modulus calculated from Equation 15, versus the measured modulus, E_{exp}. The solid curves in Figs 7 and 8 represent the trace of values for which $E_{cal} = E_{exp}$, that is, the solid line indicates an ideal fit of the data to the model. The distance from the solid line to a particular data point (Figs 7 and 8) measures the difference between the data and the model's predicted value. For both the super glue and the epoxy cement adhered composite specimens, the

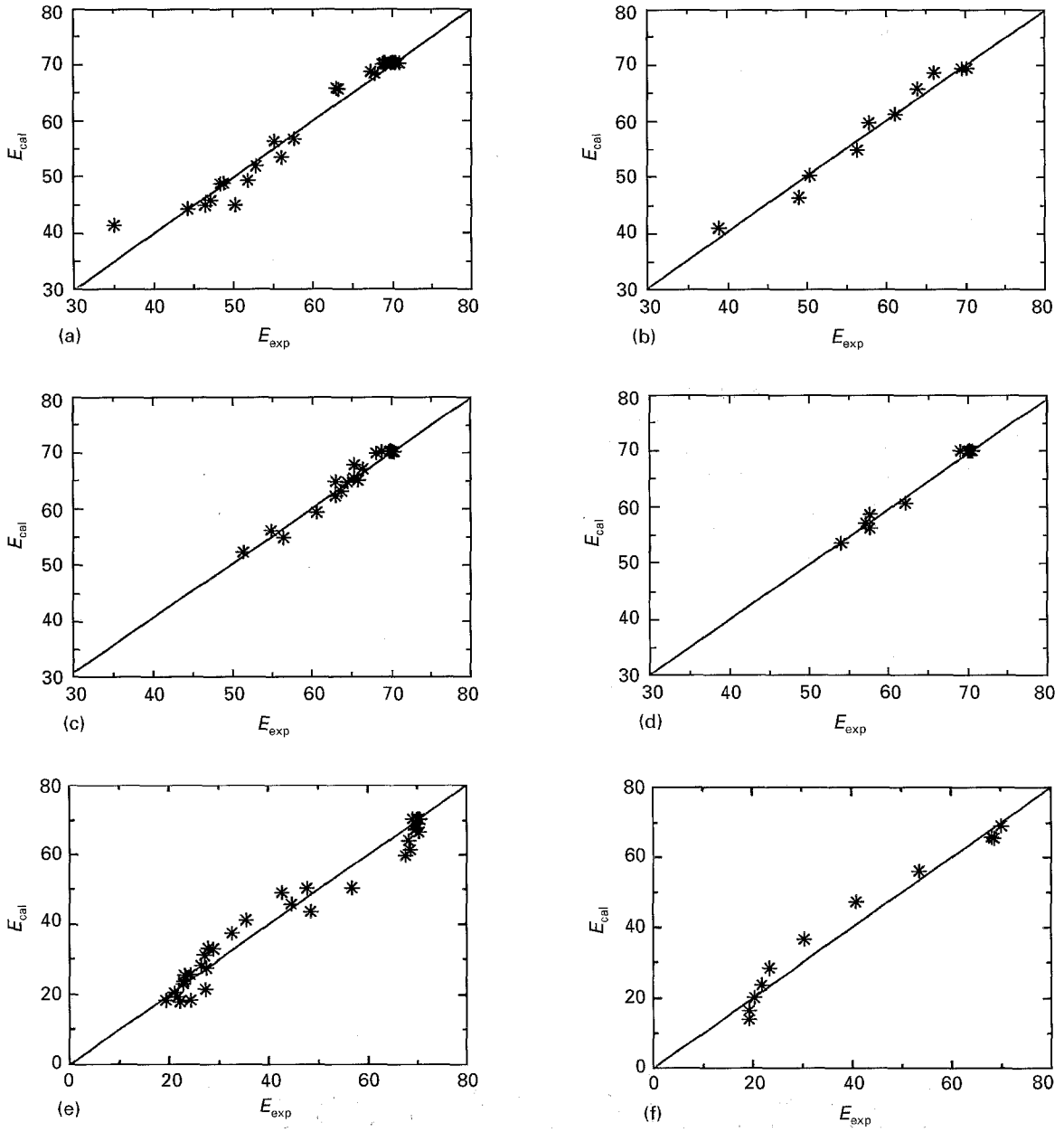

Figure 7 Measured Young's modulus versus the Young's modulus calculated from Equation 15 depending on the number of glue spots for each set of (a, c, e) super glue or (b, d, f) epoxy cement adhered composite specimens. Number of spots: (a, b) 3, (c) 2, (d) 5, (e, f) 1.

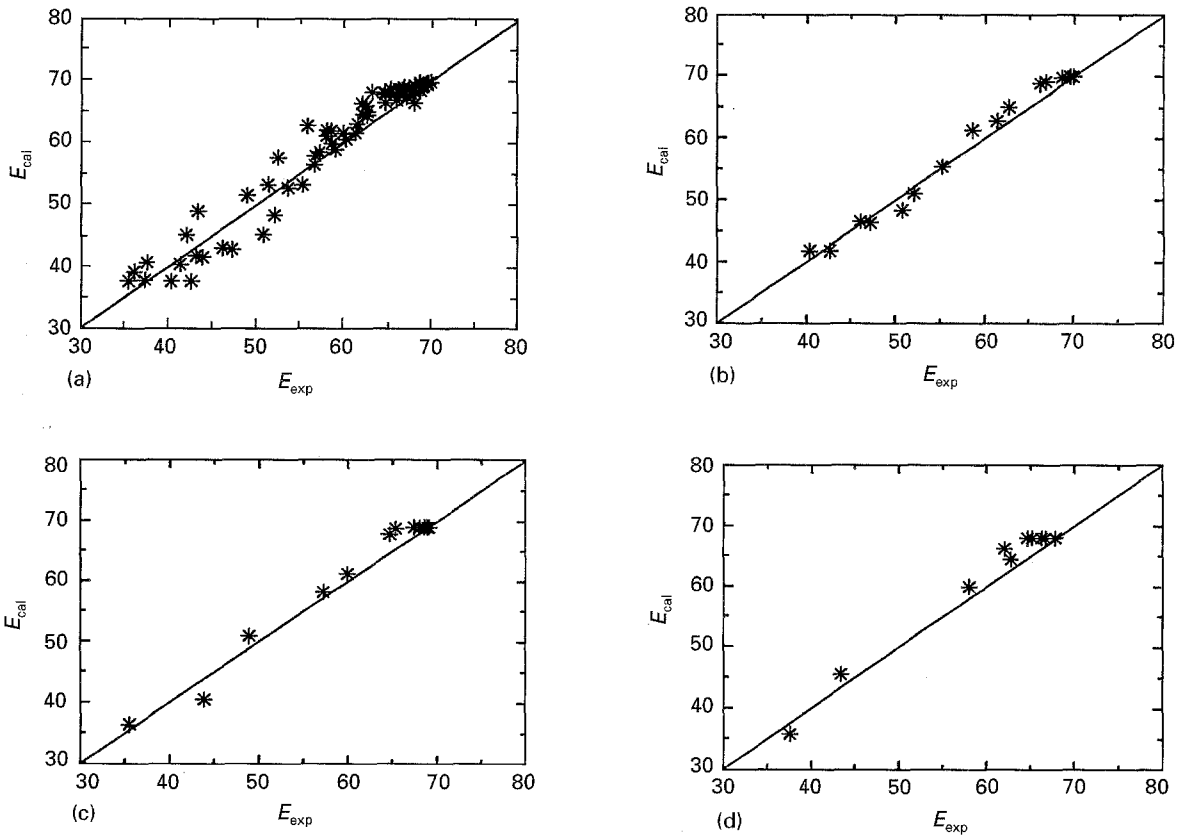

Figure 8 Measured Young's modulus versus the Young's modulus calculated from Equation 15 for each set of epoxy resin adhered composite specimens having three glue spots. (a) 0.036–0.370 mm, (b) 0.025–0.075 mm, (c) 0.125–0.175 mm, (d) 0.225–0.275 mm.

modulus values calculated for one glue spot (Figs 7e and f) show relatively more scatter than the modulus values calculated for two or more glue spots (Figs 7a–d). For the entire set of 70 epoxy resin adhered composite specimens having three glue spots and bond thicknesses ranging from 0.036–0.370 mm (Part I, Table I [1]), the difference between the measured modulus and the modulus predicted from Equation 15 was greater than 5% for 25 of the seventy specimens (Table III) (Fig. 8a). For 4 of those 25 specimens, the relative errors between the predicted and experimental data exceeded 10% (Table III). However, considering the entire data set, the errors are relatively uniformly distributed (Fig. 8a). The modulus values calculated for three subsets of composite specimens having different bond thickness ranges (R1 0.025–0.075 mm, R2 0.125–0.175 mm, and R3 0.225–0.275 mm) show less scatter (Fig. 8b–d).

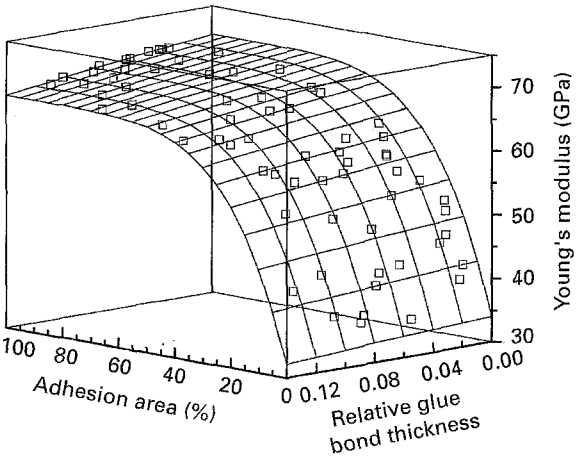

Figure 9 Three-dimensional plot of the measured Young's modulus for the 70 epoxy resin adhered specimens having three glue spots included in this study (□). The surface plotted is calculated from Equation 15, using $E_b = 2.98$ GPa and $E_g = 70.53$ GPa (Section 2.3) for $0 \leq t_R \leq 0.14$ and $0 \leq X \leq 1$.

2.4. Three-dimensional view of the model developed for glass slide/glue composite specimens

A three-dimensional plot (Fig. 9) of the measured Young's moduli for the glass slide/epoxy resin composite specimens having three glue spots shows that the 70 measured modulus values seem to be distributed above and below the surface predicted by Equation 15. For the relative bond thicknesses from 0–0.14 the model surface shows a rapid decrease in the effective Young's modulus for the adhesion areas smaller than about 40%. For the 13 epoxy resin bonded specimens having 100% adhesion area (Fig. 3) t_R was between zero and 0.12. However, for the entire set of 70 epoxy resin bonded specimens, t_R was between zero and 0.14 and the adhesion area fraction, A, varied from 0.022–1.0 (Part I, Table I [1]). The modulus surface $E(X, t_R)$ predicted from Equation 15 is shown in Fig. 10 for $0 < t_R < 1$, which is the entire physically meaningful range of the relative bond thickness. Note that for the plane defined by a fixed relative adhesion area of 100%, $E(X = 0, t_R)$ decreases from about 70.5 GPa to about 3 GPa, where 3 GPa corresponds

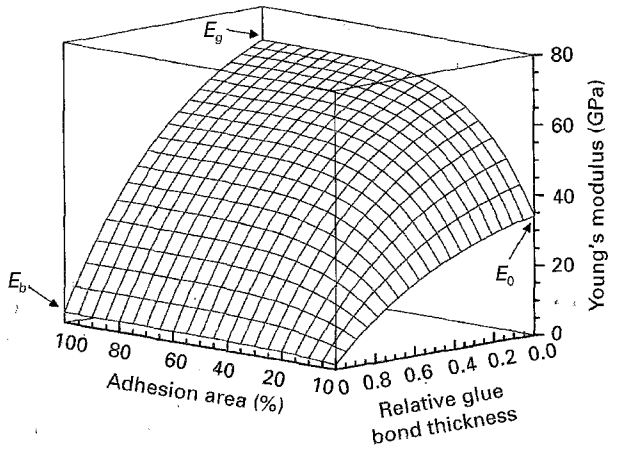

Figure 10 Three-dimensional plot of the Young's modulus predicted from Equation 15 as a function of relative adhesion area and thickness. This figure presents an extended range of relative bond thickness, namely $0 \leq t_R \leq 1$. The values of the modulus of the glass slide, E_g, and of the bond phase, E_b, are as assumed in Fig. 9, Section 2.3. E_0, the Young's modulus for specimens having no glue bond, was taken to be 34.0 GPa (Table IV), which is a value obtained from extrapolations on Young's modulus data for the seventy epoxy resin specimens included in this study (Section 2.2).

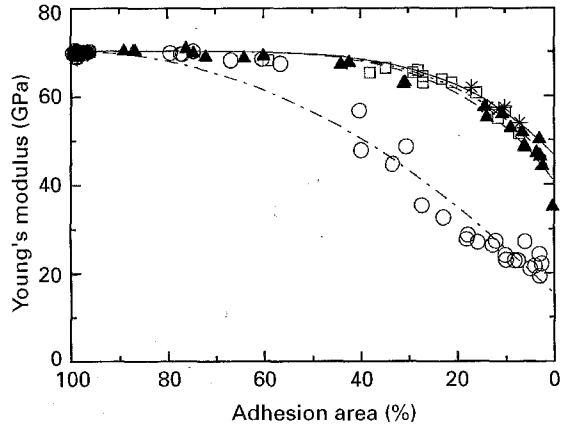

Figure 11 Application of the model developed (Equation 15) for glass slide/glue composite specimens to the super glue adhered composite specimens: (○) one glue spot, (□) two glue spots, (▲) three glue spots, (*) five glue spots.

to the modulus of the epoxy resin itself (Part I, Section 3.1 [1]). For the plane where adhesion area is fixed at 0%, $E(X = 1, t_R)$ decreases from about 35 GPa to 3 GPa.

A more conventional mode of comparing theory with experimental data is given by the two-dimensional plots displayed in Figs 11–13, where the effective Young's modulus of the glass slide/glue composite specimens is plotted as a function of the fractional adhesion area. In order to present the $E(X, t_R)$ data and models in a two-dimensional format, the mean value of t_R from each of the individual data sets was used to calculate the predicted values of $E(X, t_R)$. Table IV lists the mean t_R for each data set. The predicted $E(X, t_R)$ values, shown as the curves in Figs 11–13, were calculated from Equation 15 for the single glue spot data ($C_2 = 2$) and the multiple glue spot data ($C_2 = 5$).

The super glue and epoxy cement adhered specimens (Figs 11 and 12, respectively) are described relatively well by Equation 15. Each of the two-dimensional depictions of $E(X, t_R)$ given in Figs 11–13 represents a projection of the entire, three-dimensional data set on to the Young's modulus versus adhesion area plane. (If we project the data in Fig. 9 on to the front face of the cube depicted in that figure, then we obtain the data plot for Fig. 13). The data for the super glue and epoxy cement adhered specimens show relatively little scatter about the predicted curve, presumably in part because of the relatively restricted range of bond thickness for these two bond types (see Part I, Table I [1]). For the epoxy resin, the effect of the range of t_R values can be partially addressed by grouping the data according to thickness ranges and plotting E versus the fractional adhesion area for the individual t_R ranges (Fig. 14).

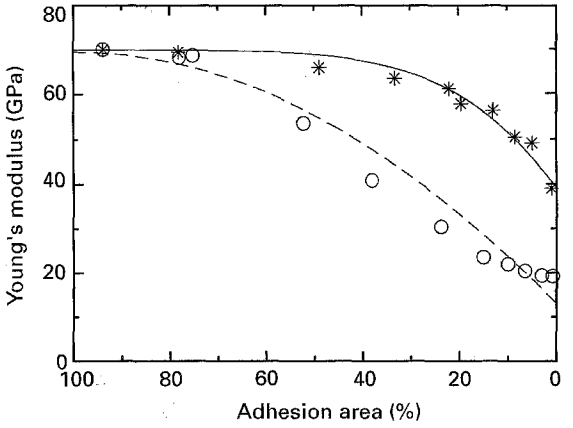

Figure 12 Application of the model developed (Equation 15) for glass slide/glue composite specimens to the epoxy cement adhered composite specimens: (○) one glue spot, (*) three glue spots.

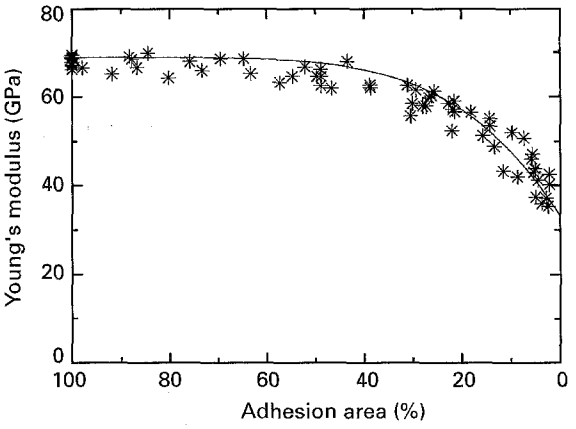

Figure 13 Application of the model developed (Equation 15) for glass slide/glue composite specimens to the epoxy resin adhered composite specimens.

3. Conclusions

The purpose of this study was to address, for a simple (i.e. "model") laminate composite system, questions such as how can we non-destructively assess the integrity of a bond layer sandwiched between two layers and what effects do imperfect adhesion have on the mechanical properties such as elastic modulus? The model laminate composite specimens included in this

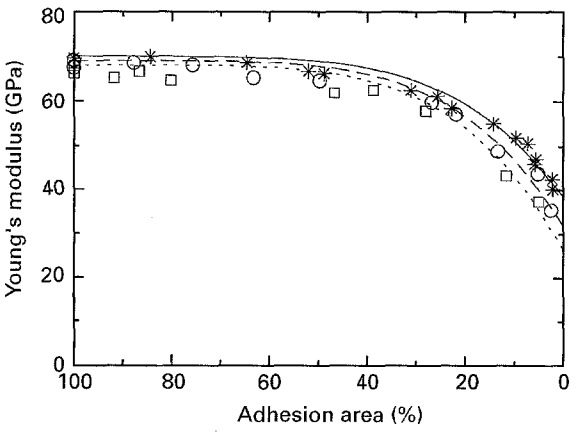

Figure 14 Effect of bond thickness described by the model developed (Equation 15) for glass slide/glue composite specimens with epoxy resin: (*) 0.025–0.075 mm, (○) 0.125–0.175 mm, (□) 0.225–0.275 mm.

study consisted of a glue bond layer sandwiched between two glass microscope slides. Three different adhesive types were used: (1) super glue, (2) epoxy cement, and (3) epoxy resin. The sonic resonance technique (Part I [1]) was used to measure the effective elastic modulus for a total of 168 glass slide/glue composite specimens, including 78 super glue adhered specimens, 20 epoxy cement adhered specimens, and 70 epoxy resin specimens (Part I, Table I [1]). The sonic resonance technique also was used to measure the modulus of three specimens fabricated entirely from epoxy resin (Part I, Fig. 2 and Tables II and III [1]), which were included to determine the modulus of that particular bond phase.

For the glass slide/glue composite specimens included in this study, the Young's modulus of the composite specimens was determined as a function of (1) relative adhesion area, (2) spatial distribution of the bond phase, and (3) relative bond thickness. For the three parameters (relative adhesion area, spatial distribution of the glue, and glue thickness), the most dramatic changes in Young's modulus were observed as a function of the relative adhesion area, for relative adhesion areas from nearly 0–70% (Figs 11–14).

In addition to the modulus changes observed as a function of adhesion area, the spatial distribution of the bond phase affected the effective modulus in the following manner: for fractional adhesion areas from 70% down to 0%, the effective modulus decreases much more rapidly for specimens adhered with one glue spot than for specimens adhered by two, three, or five glue spots (Figs 11–14). (The placement of the single and multiple glue-spot patterns is shown in Fig. 1, Part I [1]).

The effects of glue bond thickness were studied using epoxy resin adhered glass slide/glue composite specimens having a fractional adhesion area of 100%. Because the modulus of the glass slides and the bond phase had each been measured directly and because there were no adhesion area effects (the relative bond area was 100% in each case), the ROM and dynamic modulus models were used to test the data. Neither the ROM or dynamic modulus model fit the data, so using considerations of physical boundary conditions, an alternative functional form was developed for $E_{100}(t_R)$, namely

$$E_{100}(t_R) = E_g + (E_b - E_g)\, t_R \frac{\exp(t_R)}{\exp(1)} \quad (11)$$

To make further progress, we let $E(X, t_R) = E_{100}(t_R)\, E(X)$, assuming that $E(X, t_R)$ was a "separable" function. For $E(X)$, we took the empirical power-law function for $E(X)$ that had been found to fit the data well (namely $E(X) = 1 - C_1 X^{C_2}$) and again applied considerations of physical boundary conditions to determine C_1, one of the two free parameters. The resulting expression (Equation 15) for $E(X, t_R)$ was

$$E(X, t_R) = \left[E_g + (E_b - E_g)\, t_R \frac{\exp(t_R)}{\exp(1)}\right] \left[1 - \left(1 - \frac{E_0}{E_g}\right) X^{C_2}\right] \quad (15)$$

The exponent C_2 was determined on the basis of which integer in the range 2–6 gave the minimum value of $\varkappa^2$. A value of $C_2 = 2$ best described the data for glass slide/glue composite specimens adhered by one glue spot, while $C_2 = 5$ described the data for glass slide/glue composite specimens adhered by multiple glue spots. For the differing values of C_2 ($C_2 = 2$ for one glue spot, $C_2 = 5$ for multiple glue spots), the value for E_0 was determined based on the measured data of a composite specimen which gave a least value of $\varkappa^2$ in each set of composite specimens.

Equation 15 incorporates E_g (the glass slide modulus), E_b (the glue bond modulus), E_0 (the modulus for a glass slide pair having no glue bond), t_R (the relative bond thickness), and X (where X = 1 − A, and A = fractional adhesion area) in a manner that is consistent with a number of physical boundary conditions (Section 2.2). The spatial distribution of the bond phase enters the equation only through the choice of the exponent C_2. Thus a single equation (Equation 15 with $C_2 = 5$) describes well the data for all of the glass slide/glue composite specimens having multiple glue spots and the same equation (with $C_2 = 2$) describes the behaviour for glass slide/glue composite specimens having one glue spot.

Future research should examine the effective moduli for differing spatial patterns of glue spots and perhaps a greater number of glue spots (greater than five, the maximum number of glue spots used in this study). In this way, one could determine whether or not the data for a greater number of glue spots (say 10 or 50) clustered together in the manner that the multiple glue spot data (for two, three, and five glue spots) did in the present study. Also, the large mismatch between the glass slide modulus, E_g, and the glue bond modulus, E_b, makes Equation 15 relatively insensitive to the particular value of E_b. Thus further research should be done that includes E_g/E_b ratios that differ from the value of about 23 that was the case in the

present work. Also, a greater range of relative bond thicknesses would provide a more complete test of Equation 15, although the range of relative bond thicknesses included in the present study is probably adequate to represent the relative bond thicknesses employed in most practical applications of laminate composites. Also, in this study the neutral plane of the composite specimens passed through the bond phase. If Layers 1 and 2 (Fig. 2) had differing moduli and/or thicknesses, then the neutral plane could be shifted away from the bond phase. As a consequence, the effective Young's modulus might be more sensitive to bond layer defects (because the bond layer would experience greater strains in bend, for example).

Acknowledgements

We thank Brett Wilson, graduate student, Michigan State University, for his careful reading and suggestions on the final drafts of both Parts I and II of this study.

Appendix 1. Possible physical mechanisms for the deviation of experimental data from the Dynamic Modulus and the ROM models for specimens having 100% adhesion area

Several types of mechanisms could potentially explain the differences (Figs 3 and 4) between the experimental data and the theoretical predictions of the ROM and the dynamic modulus models. Firstly, the deviation between the experimental modulus values and the values predicted from the dynamic modulus model could stem from the large difference in stiffness between the glass slide layers and the glue bond layer. For our laminated glass slide/glue composite specimens, the difference in stiffness can give rise to a piecewise linear (as opposed to a linear) variation of in-plane displacement through the specimen thickness [14, 15]. Thus, the Bernoulli–Euler assumptions are less valid as the glue bond thickness increases. Therefore, the deviation should increase with increasing the glue bond thickness. A numerical analysis of the piecewise linear theory [15] as it applies to our data is currently underway [14].

The deviation of the measured elastic moduli from the moduli predicted by the ROM and the dynamic modulus models may involve imperfect interfacial bonding between two glass slides. If an actual adhesion area is less than the value of 100% that is assumed, the effective modulus of the specimens would be lower than predicted by the ROM and the dynamic modulus models assuming the experimentally determined adhesion area of nominally 100%. However, as far as we could determine via optical microscopy, the interfaces of our specimens were well adhered, except for some minor amounts of porosity in the bond phase (Part I, Appendix 2, [1]). Thus, we believe that imperfect interfacial bonding is not a significant effect for specimens included in this study.

While the glass slides do behave elastically as assumed in the ROM and the dynamic modulus models, the epoxy resin bond layer might not behave elastically, resulting in the deviation of the measured modulus from both the models. Also, unlike the ROM model, the loading in this study was not a uniaxial loading but a free–free suspension vibration by sonic resonance technique. However, the sonic resonance modulus measurement technique employed in this study is appropriate to the assumptions made for the dynamic modulus model.

Finally, the elastic modulus of the glass slide itself may shift due to residual stresses induced by shrinkage of the bond layer. Several investigators have reported stress- (or pressure-) induced changes in elastic modulus of glass or crystalline ceramics in the literature. Vega and Bogue [16] measured residual stresses in thermally quenched polymer glasses via residual optical birefringence, and reported a decrease of elastic modulus as a function of the quench medium temperature. The pressure dependence of elastic stiffness has been reported for crystalline ceramics such as magnesium oxide, sodium chloride, potassium chloride and quartz [17–19] although the effects are relatively small for crystalline ceramics. Anderson and Andreatch [17] observed that an elastic stiffness of single-crystal magnesium oxide increased by up to 20 MPa (0.66%) on increasing the hydrostatic pressure from 1 atm to 20 MPa at 23° C. In addition to the stress- (or pressure-) induced change in elastic modulus, Mallinder and Proctor [20] reported that the elastic modulus, E, of soda-glass changed under tensile loading as a function of ε, the static strain, such that $E = E_i(1–5.11\,\varepsilon)$. The intrinsic, low-strain elastic modulus, E_i, was 72.5 GPa. However, in the present study, we did not measure the stress or strain dependence of the bond phase.

Appendix 2. Qualitative explanation for the effect of the number of glue spots on the effective Young's modulus

Compared to specimens having two or more glue spots, the diminished Young's modulus for specimens having one glue spot (Figs 11 and 12) could stem from physical mechanisms that are unique to the specimens having one glue spot. In contrast to the specimens having two or more glue spots, the specimens adhered by a single glue spot may undergo two different types of motion while being vibrated by the driver transducer: (1) an opening and closing "duck-beak" motion (Fig. A1a), and/or (2) a rotational motion of the two adhered slides, where the rotational axis passes through the glue spot located at the centre of the specimen (Fig. A1b).

For the sonic resonance technique (Part I, Fig. 4 [1]), the elastic modulus of a prismatic bar-shaped specimen is proportional to the square of the fundamental flexural frequency (Part I, Equation 1 [1]). For glass slide/glue composite specimens having a single glue spot, the vibrational energy given by the driver transducer could be partitioned into energies for the

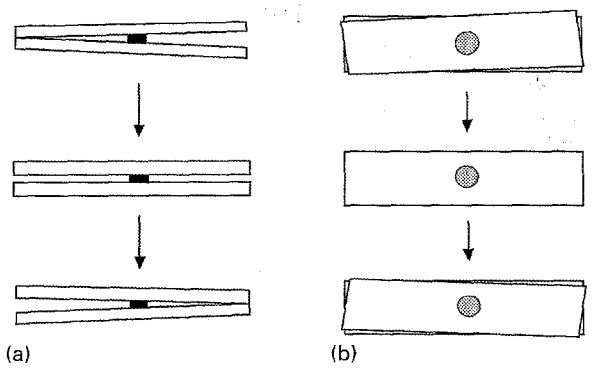

Figure A1. Schematic drawings of possible ancillary motions of the glass slide/glue composite specimens adhered by a single glue spot. (a) An opening and closing motion for the adhered glass slides (side view), (b) a relative rotational motion of the glass slides (top view).

flexural resonance as well as for the opening and closing and the rotational motions, resulting in the reduced energy for the flexural resonance (i.e. reduced fundamental flexural frequency and a reduced effective modulus) compared to the specimens having multiple glue spots. In addition, the amplitude of opening and closing and the rotational motions may increase as the adhesion area of the single glue spot located at the centre decreases from 100% to near 0%. Thus the relatively steeper decline in modulus with decreasing adhesion area for single glue spot adhered specimens, as experimentally observed in this study (Figs 11 and 12), could result from ancillary vibrations of the specimen, such as the opening and closing movement (Fig. A1a) and the relative rotational movement (Fig. A1b). However, we did not experimentally document the magnitude or even the existence of such ancillary vibrations. Thus further exploration of these effects should be a topic of a future study.

References

1. K.-Y. LEE and E. D. CASE, *J. Mater. Sci.* **31** (1996)
2. E. D. CASE and Y. KIM, *ibid.* **28** (1993) 1885.
3. E. VOLTERRA and E. C. ZACHMANOGLOU, "Dynamics of Vibrations" (Charles E. Merrill Books, Columbus, OH, 1965) pp. 321–2.
4. S. K. CLARK, "Dynamics of Continuous Elements" (Prentice Hall, Englewood Cliffs, NJ, 1972) pp. 75–87.
5. C. C. CHIU and E. D. CASE, *Mater. Sci. Eng.* **A132** (1991) 39.
6. S. P. TIMOSHENKO and D. H. YOUNG, "Strength of Materials", 4th Edn (Van Nostrand Reinhold, Princeton, NJ, 1962) pp. 113–15.
7. A. H. LANDROCK, "Adhesives Technology Handbook" (Noyes, Park Ridge, NJ, 1985) pp. 55, 153, 244, 258.
8. I. SKEIST, "Handbook of Adhesives" (Reinhold, New York, NY, 1962) pp. 323-32.
9. C. V. CAGLE, "Handbook of Adhesive Bonding" (McGraw-Hill, New York, NY, 1973) pp. 3-12, 5-3, 5-4, 6-4, 6-16, 6-17, 18-5.
10. J. SHIELDS, "Adhesives Handbook", 3rd Edn (Butterworth, Boston, MA, 1984) pp. 215, 218, 246.
11. M. J. BODNAR, "Structural Adhesives Bonding" (Wiley, New York, NY, 1966) pp. 160.
12. H. LEE, "Handbook of Epoxy Resins" (McGraw-Hill, New York, NY, 1967) pp. 6–24.
13. D. HULL, "An Introduction to Composite Materials" (Cambridge Solid State Science Series, New York, NY, 1981) pp. 29.
14. R. AVERILL, (Professor) personal communication (1993).
15. M. DI SCIUVA, *J. Sound Vibr.* **105** (1986) 425.
16. J. D. L. VEGA and D. C. BOGUE, *Chem. Eng. Commun.* **53** (1987) 23.
17. O. L. ANDERSON and P. ANDREATCH, Jr, *J. Am. Ceram. Soc.* **49** (1966) 404.
18. R. A. BARTELS and D. E. SCHUELE, *J. Phys. Chem. Solids* **26** (1965) 537.
19. H. J. McSKIMIN, P. ANDREATCH, Jr and R. N. THURSTON, *J. Appl. Phys.* **36** (1965) 1624.
20. F. P. MALLINDER and B. A. PROCTOR, *Phys. Chem. Glasses* **5** (4) (1964) 91.

Received 15 September
and accepted 25 October 1995